Scientific paper

Modelling and Prediction of Permeate Flux in the Ultrafiltration Recovery of Sodium Lignosulfonate from Aqueous Solution

Vinay B. Patel^{1,2}, Haresh K. Dave², Tejal M. Patel² and Kaushik Nath^{2,*}

¹ Research scholar, Gujarat Technological University, Ahmedabad, Gujarat, India

² Department of Chemical Engineering G H Patel College of Engineering & Technology (The CVM University), Vallabh Vidyanagar-388120, Gujarat, India

* Corresponding author: E-mail: kaushiknath@gcet.ac.in

Received: 01-21-2025

Abstract

Modelling and data fitting for the prediction of permeate flux during ultrafiltration (UF) of a model feed solution of sodium lignosulfonate was carried out following resistance in series, gel polarization and Kedem Katchalsky equations. The experiments were conducted in a laboratory UF unit equipped with PES/HFUF asymmetric membrane under specific operating conditions by altering some parameters including solute concentration, transmembrane pressure (TMP), and cross flow velocity (CFV). The maximum experimental permeate flux was observed at TMP of 3.92 bar and CFV 0.527 $\rm ms^{-1}$ was $19.6\times10^{-6}\,\rm m^{3}m^{-2}s^{-1}$. The theoretical and experimental volumetric flux was plotted, and their extent of resemblance was compared and validated statistically. The study sheds light on the effective upcycling of sodium lignosulfonate from spent liquor via ultrafiltration.

Keywords: Lignosulfonate, ultrafiltration, transmembrane pressure, model, flux

1. Introduction

Spent sulphite liquor, apparently considered to be a waste stream, produced in the sulphite pulping could be a rich source of sodium lignosulfonate - an invaluable product with innumerable upcycling options. Lignosulfonates (LS) have sparked interest due to its variety of applications as surfactants, dispersants of pesticides and dyes, cement and detergent builders, binders in ceramics, tanning and ingredients of fine chemical production.^{1,2} There are multiple processing routes for the isolation and extraction of sodium lignosulfonate from commercial spent pulping liquor. The Howard process is one of the classical and widely used methods in which precipitation of lignosulfonate is accomplished by addition of excess lime. Fractionation based on solubility and molecular weight of the components includes solvent extraction, and precipitation.^{3, 4} Selective adsorption using different sorbents such as synthetic polymeric resins, sandstone, lime stone, dolomite etc. has been reported by several authors.^{1,5} Other methods include amine extraction using long chain alkali amines followed by alkali extraction, ion-exchange via exchange of sodium ion with hydrogen ion from the resin and membrane processes. 1.6.7 Despite being unique in their application and having several advantages, most of these methods have met with limited success. Adsorption is constrained by equilibrium and regeneration of spent sorbents. The same is true for ion exchange method as well, where the resin requires frequent replacement resulting in repeated plant shutdown and incurring high operational cost. Additionally, these methods are relatively tedious, and at times fail to recover a substantial quantity of LS.

In recent years, the use of semipermeable membranes, both commercial and indigenously functionalized have broadened the application of ultrafiltration (UF) in various sectors. Selective separation and fractionation of lignosulfonates from dilute spent liquor holds much promise in the development of biorefinery operations. Application of membranes with a variety of molecular weight cutoffs can shed much light on some rough, preliminary information on molecular weight distribution. Study of

earlier literature reveals that ultrafiltration could yield a significant percentage of purified LS.1 Various authors reported the combination of ultrafiltration and nanofiltration for the production of pure lignin fractions.^{8,9} Even ultrafiltration could greatly reduce the polydispersity of the purified LS.^{10,11} Fernández-Rodríguez 2015¹² carried out the fractionation of spent sulphite liquor by combining three ceramic UF membranes (molecular weight cut off of 15kDa, 5 kDa and 1kDa) in series and reported total LS rejection up to 72.56%. Parameters that affect the final product in UF comprise of trans-membrane pressure, feed temperature, cross-flow velocity, and the Reynolds number. In one of our earlier papers, ¹³we reported the feasibility of UF to concentrate sodium lignosulfonate along with the analysis of dilution factor on permeate flux and solute retention.

The design and operation of ultrafiltration system entail accurate prediction of performance and rigorous analysis in terms of specific performance parameters such as water flux (membrane throughput) and solute rejection. However, UF rejection data have been analyzed less quantitatively than flux data in pertinent literature. To that end the present work bridges a research gap. Thus, the key focus of this work was to predict the permeate flux following resistance in series, gel polarization and Kedem-Katchalsky (K-K) equations and to compare the resemblance of experimental and predicted flux following statistical validation. These phenomenological models incorporate some of the important hallmarks of membrane separation, such as concentration polarization and formation of gel layer along with illustration of mass transfer across membrane. Modelling was carried out assuming that each of the hydraulic, osmotic pressure and concentration polarization resistances was dependent on the operating conditions. Modelling and data fitting was carried out by writing a program using Google Colab Python 3.10 version following resistance in series, gel polarization and Kedem Katchalsky equations.¹⁴ It is expected that the results and model of the present study will be advantageous in a wide spectra of UF applications and facilitate commercial leverage at higher scale. Although the present experimental study is limited to the beneficiation of sodium lignosulfonate from dilute solution, the model used herein would certainly be applicable to other feed solutions within the framework of well-defined physical properties.

2. Materials and Methods

2. 1. Chemicals and Membranes

A hydrophilic commercial ultrafiltration membrane made of polyether sulfone was selected in the present experiment. It was supplied by M/s Aquaneel Separation Pvt Ltd, Vadodara, India. The molecular weight cut off the membrane was 5 kDa with maximum operating temperature 45 °C and pH range being 1–14. Distilled water of

conductivity in the range of 10– $15~\mu s~cm^{-1}$ was used to prepare reagents. Various chemicals including sodium lignosulfonate (SLS, 96%) involved in experiments were of AR grades purchased from Merck Limited, Mumbai, India. The chemicals were used as purchased without any further treatment. The permeability of the membrane was evaluated after plotting permeate flux against trans-membrane pressure (TMP) using distilled water at ambient temperature.

2. 2. Ultrafiltration Study of Lignosulfonate Solution

Ultrafiltration of model feed solution of sodium lignosulfonate was carried out in a laboratory scale UF system. The schematic description of the experimental set up is given elsewhere. 13 A polyether sulfone flat sheet membrane with molecular weight cut off 5 kDa was used. LS feed solution was prepared by dissolving suitable quantity (the range being 1.2 to 1.24 g l^{-1}) of sodium lignosulfonate powder in deionized water. While evaluating the effect of selected operating conditions on model parameters, a number of experimental measurements were carried out at varying cross flow velocity and trans membrane pressure. The flux measurement study was carried out at four different cross flow velocities (ms-1) like 0.323, 0.357, 0.425 and 0.527. The experimental flux calculation was carried out at four different trans-membrane pressures, namely 1.96, 2.94, 3.92 and 4.9 bar. The used membranes were cleaned using distilled water after each measurement followed by chemical cleaning, with EDTA (0.8% (w) of Na-EDTA (sodium salt of ethylaminediamine-tetraacetic acid) and detergent solution (2.0% (w) of STPP (sodium tripolyphosphate) $(Na_5P_3O_{10})$ and 0.025% (w) Na-DDBS (C₆H₅(CH₂)₁₂-SO₃Na) (sodium salt of dodecylbenzene sulfonate).

2. 3. Concentration of the Feed, Permeate and Reject Stream

The concentration of feed solution, permeate solution and reject solution was determined using a UV–VIS spectrophotometer (Model: Lambda 19, Perkin Elmer, USA) in a linear absorbance mode (scan speed 0.3–1200 nm min⁻¹, resolution 0.8 nm, deuterium lamp) out at a wavelength of 280 nm.

2. 4. Permeability and Flux Measurement of Membrane

The permeability of the used membrane was determined at various operating pressure using deionized water. The membrane permeability was determined from the slope of the permeate flux against trans-membrane pressure plot. The pure water flux $J_{\rm w}(m^3m^{-2}\,s^{-1})$ was calculated using Eq. (1)

$$J_{w} = V/At \tag{1}$$

Where V is the volume of the permeate sample (m³), A is the effective area (m²) and Δt is the permeation time (s). The experiments were carried out at room temperature and average of three reading was reported.

2. 5. Modelling of the Present Study

Resistance in series model

Resistance in series model quantifies a number of mass transfer resistances during membrane transport. Total resistance Rtot can be expressed by Eq. (2).^{15,16}

$$R_{tot} = R_m + R_{ad} + R_{cp} + R_p \tag{2}$$

 R_{mp} , R_{adb} , R_{cp} and R_p were calculated following the method described elsewhere. The model was developed using principles of solution-diffusion and film theory and correlation for concentration polarization resistance. The transport equation through the porous membrane can be given by the Darcy's law to describe the osmotic pressure-controlled flux (Eq. 3)¹⁸

$$Vw^{osm} = L_p(\Delta P - \Delta \pi) \tag{3}$$

Where, $Lp = (1/\mu Rm)$, which indicates the permeability of the membrane. This permeability is related to the traditional Darcy's permeability (ko) as, $Lp = ko/\mu\delta$, where δ is the thickness of the membrane skin and μ is the viscosity of the permeating solution. The osmotic pressure difference across the membrane is given by Eq. (4)

$$\Delta \pi = \pi_m - \pi_p \tag{4}$$

Osmotic pressure of feed solution at membrane surface and in the permeate was estimated by using Vant Hoff's equation considering dilute solution. Accordingly, incorporating the osmotic coefficient 'a' at room temperature and considering molecular weight of sodium lignosulfonate (average molecular weight: 534.502 g mol⁻¹; universal gas constant R: 8314 J mol⁻¹K⁻¹; T: 303 K), the osmotic pressure becomes

$$\pi = 4713. C_p \tag{5}$$

Real retention (R_r) can be defined as the ratio of difference between membrane surface and permeate concentration to membrane surface concentration. It is a constant for a particular membrane-solute system.

$$R_r = 1 - \frac{c_p}{c_m} \tag{6}$$

Using Eqs. (3) to (5), the osmotic pressure-controlled flux is expressed as

$$Vw^{osm} = L_n(\Delta P - 4713C_m R_r) \tag{7}$$

The osmotic pressure controlled flux; vw^{osm} cannot be calculated from Eq. (7), as

 C_m is unknown. For that, the film theory for steady state mass transfer (Eq. 8) is used

$$Vw^{osm}.C + D.\frac{dc}{dv} = Vw^{osm}.C_p$$
 (8)

On integrating Eq. (8) from y = 0, $c = c_{\rm m}$ to $y = \delta$, $c = c_o$, the standard film theory equation is obtained as represented by Eq. (9)

$$Vw^{osm} = kln \left[\frac{c_m - c_p}{c_o - c_p} \right] \tag{9}$$

The permeate concentration C_p can be expressed in terms of the membrane surface concentration, c_m and R_r from Eq. (6). Eq. (9) can be expressed as

$$Vw^{osm} = kln\left(\frac{c_m.R_r}{c_o-c_m(1-R_r)}\right)$$
 (10)

In general, the Sherwood (*Sh*) number is related to the Schmidt (*Sc*) and Reynolds (*Re*) numbers for laminar flow as Eq. (11)

$$S_h = \frac{k.de}{D} = 1.85 \left(Re. Sc. \frac{de}{L} \right)^{1/3}$$
 (11)

For turbulent flow conditions (Re > 2000-4000) Harriott-Hamilton correlation (Eq. 12) was used to calculate Sh.¹⁹

$$S_h = 0.0096. R_e^{0.91}. S_c^{0.35} (12)$$

Diffusivity D, was determined using the correlation of Wilke and Chang²⁰ (Eq. 13).

$$D = \frac{(117.3 \times 10^{-18})(\varphi.M)^{0.5}.T}{\mu.v^{0.6}}$$
 (13)

Combining Eq. (7) and (9), Eq. (14) was obtained

$$Vw^{osm} = L_p \left(\Delta P - 4713C_m R_r\right)$$

$$= kln\left(\frac{c_m R_r}{C_0 - C_m (1 - R_r)}\right)$$
(14)

Eq. (14) was solved using Newton-Raphson trial and error method, to determine C_m and hence Vw^{osm} . Once C_m is calculated from Eq. (14) the permeate concentration C_p can be estimated from Eq. (6). For the determination of various resistances and models parameters a schematic algorithm of Python-designed computational program is presented in Fig. 1.

Gel polarization model

The mass transfer coefficient was calculated from Sherwood number²¹ after calculating Reynold's number

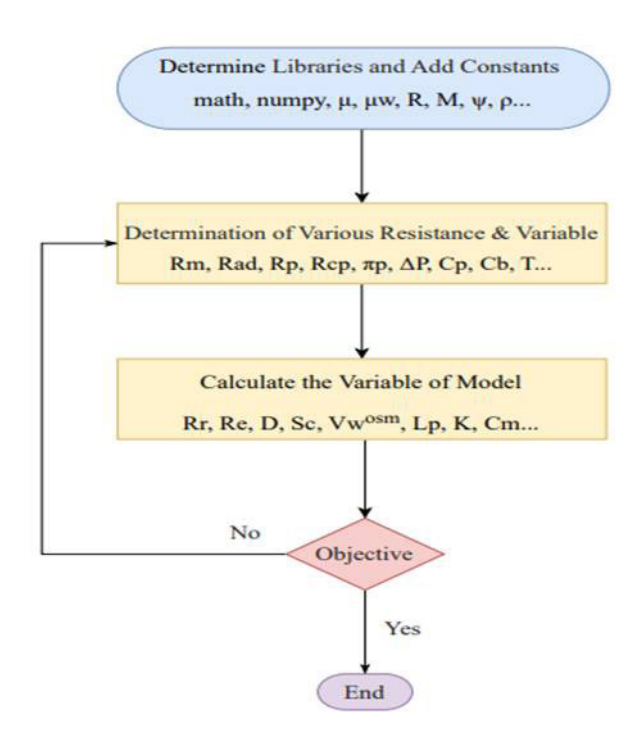


Fig. 1 Schematic algorithm of Python-designed computational program

and Schmidt number from cross flow velocity of the solution. The value of mass transfer coefficient was used to predict membrane surface concentration and then predicted flux calculation.²² The predicted flux calculation from gel polarization model compared with experimental flux calculation.

$$R_{obs} = 1 - \frac{c_p}{c_o} \tag{15}$$

$$J = k ln \left[\left(\frac{c_m - c_p}{c_o - c_p} \right) \right] \tag{16}$$

$$C_m = C_p + \left(C_o - C_p\right) \exp\left(\frac{I}{k}\right) \tag{17}$$

$$S_h = 0.023 \text{Re}^{0.875} Sc^{0.25} \tag{18}$$

Kedem Katchalsky Model

Pure water permeability (L_p) was calculated by doing the experiments at different TMP. The predicted solvent flux was calculated by Eq. (19) 23 and compared with experimental flux. The reflection coefficient was assumed to be 0.9.

$$J = L_p(\Delta P - \sigma \Delta \pi) = \text{Solvent flux}$$
 (19)

Where $\Delta \pi = RT(C_o - C_p)$. Incorporating Eq. (17) in Eq. (19) and substituting $\Delta \pi$ solvent flux was estimated.

2. 6. Statistical Analysis

The difference between measured or estimated value and the true value was expressed as a ratio of the absolute difference to the true value.

$$Relative Error = \frac{|True \, Value - Measured \, Value|}{True \, Value}$$

Root mean square error can be estimated following Eq. (20), in which the smaller the value of RMSE, the better will be the fit between the predicted and experimental data

$$RMSE = \sqrt{\frac{1}{N} \sum_{i=1}^{N} (J_{i,exp} - J_{i,theory})^2}$$
 (20)

Where RMSE = Root mean square error

Chi-square test is a statistical analysis used to compare actual results with an expected hypothesis. It combines both curve-fitting and model testing by considering measurement uncertainties following Eq. (21).

$$x^{2} = \sum \frac{(O_{i} - E_{i})^{2}}{E_{i}}$$
 (21)

Where O_i = observed value and E_i = expected value

A smaller value of x^2 is indicative of good fit of model data with those of experimental.

3. Results and Discussion

Membrane flux or throughput is an important performance index for any pressure driven membrane process including UF. Forecasting of permeate flux is an important consideration for long-term UF operation. Membrane durability as well as permeate flux is influenced by the phenomena named concentration polarization (i.e., solute build-up) and fouling (due to adhesion of microbial cells, solute particles, gel layer formation etc.) at the membrane surface. Similar to other filtration process UF is also encountered with the drop of permeate flux largely due to aforementioned factors. 24,25 In the present study, prior to modelling of permeate flux, effect of trans-membrane pressure on it and its time evolution under specific experimental conditions were investigated. Later, three mathematical models namely resistance in series, gel polarization and Kedem-Katchalsky (K-K) were applied. Predicted flux estimated from these three models was then compared with experimental flux. These are highlighted in the following subsections.

3. 1. Effect of Trans-membrane Pressure

It was observed in the present experiment, that permeate-flux increased proportionally with the trans-membrane pressure within the pressure range studied in all cases. This implies that the operation was within the pressure-controlled region. Fig 2 represents the experimental permeate flux as a function of trans-membrane pressure at four different cross flow velocities for a run time of 60 min and at constant initial feed concentration of 1.24 gL $^{-1}$. A perusal of Fig 2 reveals that at 3.92 bar pressure, experimental flux was found to be maximal for all cross flow velocities. At a cross flow velocity of 0.527 ms $^{-1}$ the values of permeate flux were estimated to be 13.4 \times 10 $^{-6}$ and 17.4 \times 10 $^{-6}$ m 3 m $^{-2}$ s $^{-1}$ at trans-membrane pressure of 2.94 and 3.92 bar respectively.

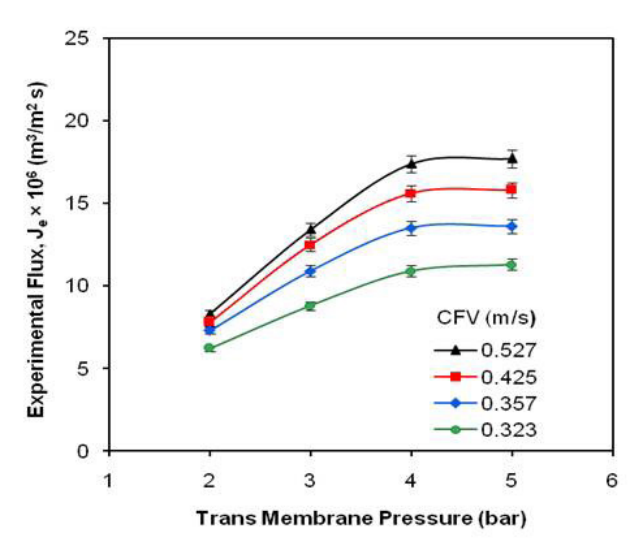


Fig. 2 Experimental flux as a function of trans-membrane pressure at various cross flow velocities (Feed concentration: 1.24 g/L; run time: 60 min, temp: ambient).

The figure also indicates that increase in cross flow velocity resulted in substantial flux improvement. For example, at CFV of 0.323m s⁻¹, the maximum permeate flux at 3.92 bar TMP was found out to be 10.9×10^{-6} m³ m⁻²s⁻¹ and this rose to $17.4 \times 10^{-6} \text{ m}^3 \text{ m}^{-2} \text{s}^{-1}$ when CFV was increased to 0.527 ms⁻¹ thereby, registering a 59.6% increase. A higher cross flow velocity can effect a sweeping action across the membrane, minimizing the concentration gradient towards the membrane surface and subsequently results in flux increment.²⁵ As the trans-membrane pressure increases, the osmotic pressure also increases, which can partly nullify the increase in flux. Thus, beyond 3.92 bar pressure there was negligible increase in permeate flux. It means the attainment of the "critical flux" region of UF, which is where the flux starts to plateau. At this point, further increasing the pressure generally does not augment the flux. These observations follow the similar trend as reported by Bhattacharya et al (2005)²⁷ for the ultrafiltration of sodium lignosulfonate from spent sulphite liquor. Our study indicates that 3.92 bar trans-membrane pressure was found to be the most appropriate under the present experimental conditions.

3. 2. Time Evolution of Permeate Flux

Fig 3 represents the experimental flux as a function of time for a feed solution having initial concentration of 1.24 gL⁻¹, and TMP 3.92 bar at four different cross flow velocities (CFVs). At CFV of 0.527 ms⁻¹, and transmembrane pressure of 3.92 bar permeation flux was estimated to be 19.6×10^{-6} m³ m⁻²s⁻¹ after 15 min of operation which however reduced to 17.4×10^{-6} and 15.2×10^{-6} m³/ m⁻²s⁻¹ after 45 and 60 min respectively. This corresponds to 28.9% reduction of initial flux. For other cross flow velocities the percentage flux reduction was in the range of 25–28% under similar experimental conditions.

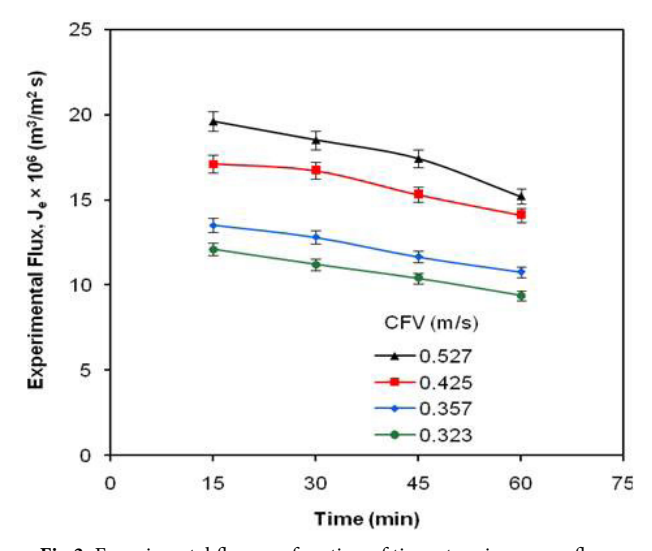


Fig 3. Experimental flux as a function of time at various cross flow velocities (Feed concentration = 1.24 g/L; trans membrane pressure: 3.92 bar, run time: 60 min, temp: ambient)

The declining trend of permeate flux with time, as shown in Fig 3, is ascribed to the phenomenon of solute build up (concentration polarization) on the surface layer of membrane imparting resistance to solvent transport.

Although concentration polarization could be reversible during the initial period of operation, it becomes irreversible phenomena like solute adsorption and gel layer. A perusal of the profile of permeate flux as a function of time indicates gradual decline of flux with time. Initially the decline was sharp followed by a steady decline in line with the classical filtration theory. At the beginning of operation smaller solutes presumably block the membrane pores resulting in flux decline, which further aggravated due to gradual concentration polarization on the membrane surface. It has been reported by many authors that resistance arising out of the concentration polarization is the dominating cause for the permeate flux decline reaching values somewhat two times higher than the hydraulic membrane resistance. 28,29 At the end of each experimental run, the used membrane was thoroughly washed and reused. It was found that original membrane permeability could be largely regained. This possibly indicates that the

Table 1: Comparison with similar other studies of ultrafiltration of spent sulfite liquor from literature

Sr No	Membrane types and features	Average permeate flux (L/m² h)	Trans membrane pressure (bar)	Major findings	Reference	
1	TiO ₂ ceramic membranes are used (MWCO: 1, 5 and 15 kDa)	55.45, 5.77 and 6.00 for 15, 5 and 1 kDa membranes respectively	1.8 to 2.0	Fractionation of spent [12] sulfite liquor into monomeric sugars and LS. Highest LS rejection (65.68 %)		
2	Polysulfone membrane (GR 60-P)	Not presented	6.0 to 11.5	Concentration polarization model was used to determine lignosulfonate rejection. Average molecular mass was also estimated	[21]	
3	Polysulfone and fluoropolymer membranes (MWCO 10–100 kDa)	100–700 (a wider range for different membranes	0 to 10	High MWCO GR membranes are very suitable for UF of SSL for the recovery of lignosulphonates.	[27]	
4	Ceramic hollow fiber membranes with MWCO 20 kDa, 20 kDa, 30 nm, 8 nm, and 3 nm	252 to 261	3.0 to 7.0	Ceramic hollow fiber membrane were comparable and even better than tubular membrane to concentrate spent sulfite liquor	. r	
5	Polysulfone, polyethersulfone and fluoropolymer composite membranes (MWCO:1–10 kDa)	10 to 50	2 to 5	Could not fractionate lignosulphonates from sugars due to overlapping molecular weights of LS and sugars	[31]	
6	Polyether sulfone membrane (MWCO: 5 kDa)	13.4 to 17.4	1.9 to 4.9	Modelling and data fitting was carried out following RIS, GP and K-K equations.	Present study	

fouling due to pore blocking was reversible. Additionally, Table 1 summarizes the comparison of major experimental findings from similar other studies of ultrafiltration of spent sulfite liquor from pertinent literature.

3. 3. Experimental and Predicted Flux Using Various Models

Predicting the permeate flux is critical for evaluating and optimizing the performance of the ultrafiltration process. In modelling, along with model description it is vitally important to analyse and validate the capacity of the models to predict the permeation flux. This, in turn, impacts the further use of these models for scaling up to industrial level. In the present study three models namely resistance in series, gel polarization and K-K were applied for predicting flux of permeate in ultrafiltration of sodium lignosulfonate solution. Fig 4 presents graphical comparison of the theoretically predicted versus experimentally determined volumetric permeate flux using three different models at four different cross flow velocities (CFV). A perusal of Fig 4 indicates that theoretically predicted permeate flux following resistance in series and gel polarization models, conforms more closely to the experimental values compared to K-K model.

Theoretically, the resistances against solvent flux are the summation of the membrane hydraulic resistance, reversible pore-blocking resistance, and a deposited gel-layer resistance. Using K-K model, predicted flux values become exorbitantly higher than those of experimentally determined ones. The extent of matching between the predicted permeation flux and the experimental data, following all the three models was evaluated using statistical performance parameters such as root mean square error (RMSE), chi square test, and percentage relative error (RE) (Table 2). The smaller the values of RMSE and RE, the better would be the matching between the predicted and the experimental fluxes. The same is true for the chi square test as well. Thus, from a further observation of Table 1, it is evident that at a cross flow velocity of 0.527 ms⁻¹, RMSE, RE and chi squared parameters are minimal for resistance in series and gel polarization models. It also indicates that increase in cross flow velocity resulted in a marginally better fit between experimental and predicted flux values. The highest relative error and root mean square errors (in bracket) estimated for the predicted permeate flux using resistance-in-series, gel polarization and K-K models were 0.603 (6.765), 0.684 (7.640), 2.892 (30.292) respectively. The results obtained, within the statistically validated models, showed that K-K model presents a high variability of prediction (values of percentage relative error in the range of 2.89-3.32), and root Mean Square Error (RMSE) in the range of 26.53-30.29 within the experimental framework. The chi square test analysis also shows that x² values for curve fitting by using resistance in series and gel polarization models are very low

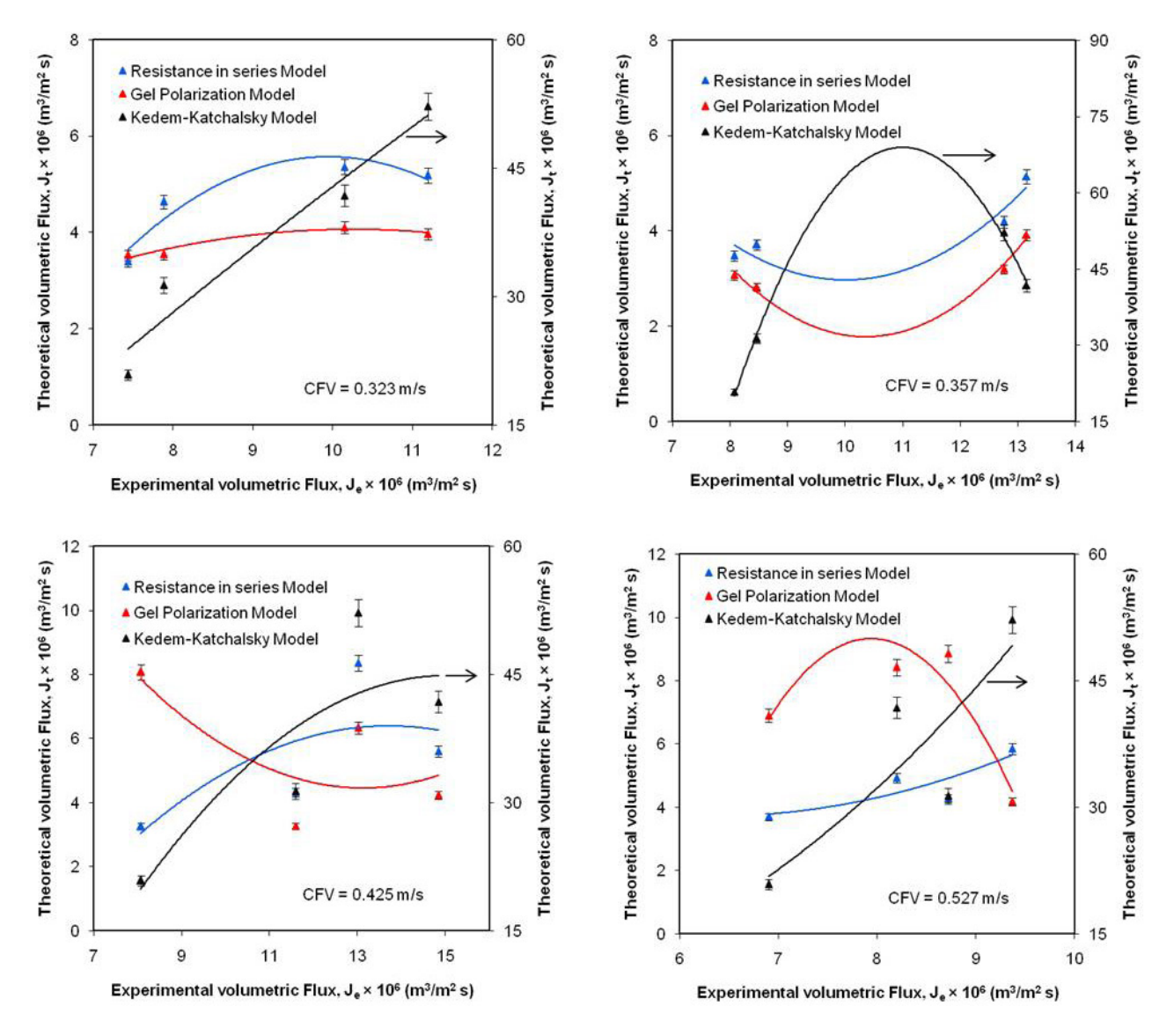


Fig 4: Graphical comparison theoretical Vs Experimental volumetric flux using three different models at four different cross flow velocities (CFV). (a) CFV: 0.323 m/s (b) CFV: 0.357 m/s (c) CFV: 0.425 m/s (d) 0.527 m/s; (Feed concentration = 1.24 g/L; trans membrane pressure: 3.92 bar; run time: 60 min, temp: ambient).

compared to those obtained in K-K model for all the cross flow velocities.

The significant deviation between the experimental data and those predicted by the K-K model might be due to fluctuating interference of the operating parame-

ters and experimental inaccuracies. Kedem-Katchalsky equations are based on the linear thermodynamics of irreversible processes. The equations are valid for membrane systems with two-component solutions, suitably diluted and well stirred. Since, under the present experimental set

Table 2: Statistical analysis of goodness of fit between experimental and predicted volumetric flux of ultrafiltration SLS solution (*Resistance in series: RIS; Gel Polarization: GP; Kedem-Katchalsky:KK*)

CFV	Chi square			RMSE			% RE		
(m/s)	RIS	GP	KK	RIS	GP	KK	RIS	GP	KK
0.323	4.312	1.700	21.394	4.633	5.542	29.216	0.491	0.579	2.892
0.357	4.153	1.748	23.992	6.732	7.640	27.676	0.603	0.684	2.390
0.425	3.175	1.648	17.009	6.765	7.519	26.534	0.551	0.486	2.029
0.527	1.604	1.4	7.833	3.636	2.592	30.292	0.436	0.128	3.322

up the feed solution was not sufficiently well stirred, the K-K model showed a deviation from the predicted values. In literature mostly it is applied for RO and NF systems, where applied pressures are relatively high. The reason why two proposed models worked well, whilst the other fared poorly is not obvious at this stage. Nevertheless, there is a strong likelihood of other forms of membrane-solute interaction which was not investigated in the present work. In future, another form of interaction should be taken into account. In essence, the findings of data fitting show that the osmotic pressure difference, the cross-flow velocity of the feed solution, and the water permeability coefficient has a significant impact on water flux.

4. Conclusion

The performance of the resistance in series and gel polarization model, studied in our work for the prediction of permeate flux is quite satisfactory, since the model predictions are in consonance with the experimental data. In both of these models statistical fit parameters such as root mean square error, percentage relative error and chi square test values were estimated to be in the lower range compared to Kedem Katchalsky model thereby indicating conformation between theoretical and experimental flux data. However, Kedem Katchalsky model represents substantial difference between experimental and theoretical values. However, the phenomenological models used in this study, despite presenting a moderate variability of prediction stand as unique tools for scaling-up and for better understanding of the UF process. The developed models may be utilized for any other ultrafiltration system and could be a useful tool for the scaling-up of processes from laboratory to pilot or industrial dimensions. In conclusion, the phenomenological models presented in this paper provide an initial framework for advancing a problem of considerable practical as well as theoretical interest. Nevertheless, the application to more complex matrices needs elaborate further investigation.

Nomenclature:

 $J = Permeate flux (m^3m^{-2} s^{-1})$

 $R_{\rm m}$ = Intrinsic membrane resistance (m⁻¹)

 R_{ad} = Adsorption resistance (m⁻¹)

 R_{cp} = Concentration polarization (m⁻¹)

 R_p = Pore blocking resistance (m⁻¹)

 R_{tot} = Summation of a number of resistances

 $Vw^{\text{osm}} = \text{Osmotic pressure controlled flux } (m^3m^{-2}.s^{-1})$

 L_p = Permeability of the membrane (m³m⁻² s⁻¹ Pa⁻¹)

 ΔP = Transmembrane Pressure drop (bar)

 $\Delta \pi$ = Osmotic pressure difference

 π_m = Osmotic pressure at the membrane surface (bar)

 π_p = Osmotic pressure at the permeate stream (bar)

 \hat{C}_p = Permeate concentration (mg l⁻¹)

 C_m = Membrane surface concentration (mg l⁻¹)

 C_0 = Feed concentration (mg l⁻¹)

R = Universal gas constant (J mole⁻¹ K⁻¹)

 R_r = Real retention

k = Mass transfer coefficient (m s⁻¹)

L = Effective membrane length (m)

 $M = \text{Molecular weight of the solvent (kg kgmol}^{-1})$

 μ = Solution viscosity (kg m⁻¹ s⁻¹)

 $v = \text{Solute molar volume (kg mol m}^{-3})$

 φ = Association factor for solvent

 $R_e = Reynolds \ number, \ ^{\rho.u.d}/\mu \ (Dimensionless)$

 S_c = *Schmidt number*, μ/ρ .D (Dimensionless)

 $S_h = Sherwood number, k.d/D (Dimensionless)$

T = Temperature (K)

 $D = Diffusivity (m^2 s^{-1})$

 d_e = Equivalent diameter (m)

 σ = reflection coefficient

 R_{obs} = Rejection observed

Declaration of Competing Interest

The authors declare that they have no known competing financial interests or personal relationships that could have appeared to influence the work reported in this paper.

5. References

1. I. Sumerskii, P. Korntner, G. Zinovyev, T. Rosenau, A. Potthast, *RSC Advances*. **2015**, *5*, 92732–92742.

DOI:10.1039/C5RA14080C

K. Nath, S.C.Panchani, T. M. Patel, H. K. Dave, V. B. Patel, K. K. Tiwari, N. Sahoo, *J. Wood Chem. Tech.* 2020, 40, 331–347. DOI:10.1080/02773813.2020.1809677

- 3. D. Tarasov, M. Leitch, P. Fatehi, *Biotech. Prog.* **2015**, *31*, 1508–1514. **DOI:**10.1002/btpr.2149
- 4. W. Fang, M. Alekhina, O. Ershova, S. Heikkinen, H. Sixta, *De Gruyter* **2015**, *69*, 943–950. **DOI:**10.1515/hf-2014-0200
- P. Fatehi, J. Chen, in: Z. Fang, Jr. R. Smith, Jr. (Eds.), Production of Biofuels and Chemicals from Lignin. Biofuels and Biorefineries. Springer, Singapore, 2016. pp.35–54.
 DOI:10.1007/978-981-10-1965-4_2
- G. E. Fredheim, S. M. Braaten, B. E. Christensen, *J. Chromat.* A 2002, 942, 191–199.

DOI:10.1016/S0021-9673(01)01377-2

- 7. K. Gawluk, A. Modrzejwska-Sikorska, T. Rębiś, G. Milczarek, *Catalysts* **2017**, *7*, 392–401. **DOI:**10.3390/catal7120392
- A. Arkell, J. Olsson, O. Wallberg, Chem. Eng. Res. Des. 2014, 92, 1792–1800. DOI:10.1016/j.cherd.2013.12.018
- A-S Jönsson, A-K Nordin, O Wallberg, Chem. Eng. Res. Des. 2008, 86, 1271–1280. DOI:10.1016/j.cherd.2008.06.003
- 10. Y. Deng, W. Zhang, Y. Wu, H. Yu, X. Qiu, *J. Phys. Chem. B* **2011**, *115*, 14866–14873. **DOI:**10.1021/jp208312a
- O. Ringena, B. Saake, *Holzforschung* 2005, 59, 405–412.
 DOI:10.1515/HF.2005.066

- 12. J. Fernández-Rodríguez, A. Garcíab, A. Coza, J. Labidi, *Chem. Eng. Trnsac.* **2015**, *45*, 553–558. **DOI**: 10.3303/CET1545093
- 13. K. Nath, V. B. Patel, H. K. Dave, S. C. Panchani, *Ind. Chem. Eng.* **2022**, *64*, 553–564.
 - DOI:10.1080/00194506.2022.2028197
- C. Quezada, H. Estay, A. Cassano, E. Troncoso, R. Ruby-Figueroa, *Membranes* 2021, 11, 368.
 DOI:10.3390/membranes11050368
- 15. C. Fersi, L. Gzara, M. Dhahbi, *Desalination* **2009**, *244*, 321–332. **DOI:**10.1016/j.desal.2008.04.046
- A. Simon, N. Gondrexon, S. Taha, J. Carbon, G. Dorange, Sep. Sci. Tecnol. 2000, 35, 2619–2637.
 DOI:10.1081/SS-100102359
- 17. T. M. Patel, K. Nath, Korean J. Chem. Eng. 2014, 31, 1865–1876. DOI:10.1007/s11814-014-0139-7
- V. Karthik, S. Das Gupta, S. De, J. Membr. Sci. 2002, 199, 29–40. DOI:10.1016/S0376-7388(01)00674-3
- 19. G. B.van den Berg, I. G.Racz, C. A. Smolders, *J. Membr. Sci.* **1989**, 47, 25–51. **DOI:**10.1016/S0376-7388(00)80858-3
- 20. R. E. Treybal,1981, Mass transfer operations, 3rd Edition, McGraw-Hill Book Company, New Delhi pp. 104–123.
- 21. K. Kovasin, H. V. Norden, *1984* Svensk Papperstidning. Reprinted from Svensk Papperstidning **1984**, *87*, 6, R44–R47

- Z. Rizki, M. Ottens, Sep. Purif. Technol. 2023, 315, 123682.
 DOI:10.1016/j.seppur.2023.123682
- J. Geens, K. Boussu, C. Vandecasteele, B. Van der Bruggen, J. Membr. Sci. 2006, 281, 139–148.
 DOI:10.1016/j.memsci.2006.03.028
- G. E. Wetterau, M. M. Clark, C. J. Anselme, J. Memb. Sci. 1996, 109, 185–204. DOI:10.1016/0376-7388(95)00200-6
- G. F. Crozes, J. G. Jacangelo, C. Anselme, J. M. Laîné, J. Memb.
 Sci. 1997, 124, 63–76. DOI:10.1016/S0376-7388(96)00244-X
- K. Katsikaris, C. Boukouvalas, K. Magoulas, *Desalination* 2005, 171, 1–11. DOI:10.1016/j.desa1.2004.02.103
- 27. P. K. Bhattacharya, R. K. Todi, M. Tiwari, C. Bhattacharjee, S. Bhattacharjee, S. Datta, *Desalination* **2005**, *174*, 287–297. **DOI:**10.1016/j.desal.2004.09.017
- D. M. Kanani, R. Ghosh, J. Membr. Sci. 2007, 290, 207–215.
 DOI:10.1016/j.memsci.2006.12.030
- C. Serra, M. J. Clifton, P. Moulin, J. C. Rouch, P. Aptel, J. Membr. Sci. 1998, 145, 159–172.
 DOI:10.1016/S0376-7388(98)00075-1
- D. Humpert, M. Ebrahimi, A. Stroh, P. Czermak, *Membranes* 2019, 9, 45. DOI:10.3390/membranes9040045
- J. A. Restolho, A. Prates, M. N. de Pinho, M. D. Afonso, *Biomass bioener*. 2009, 33 1558–1566.
 DOI:10.1016/j.biombioe.2009.07.022

Povzetek

Modeliranje in prilagajanje podatkov za napovedovanje pretoka permeata med ultrafiltracijo (UF) modelne hranilne raztopine natrijevega lignosulfonata je bilo izvedeno z zasledovanjem upora v serijah, gelne polarizacije in enačbami Kedem Katchalsky. Eksperimenti so potekali v laboratorijski enoti za UF, opremljeni s PES/HFUF asimetrično membrano, pod določenimi delovnimi pogoji z spreminjanjem nekaterih parametrov, vključno s koncentracijo topila, transmembranskim tlakom (TMP) in hitrostjo pretoka (CFV). Najvišji eksperimentalni pretok permeata je bil opažen pri TMP 3,92 bar in CFV 0,527 ms $^{-1}$, in je znašal 19,6 × 10 $^{-6}$ m 3 m $^{-2}$ s $^{-1}$. Teoretični in eksperimentalni volumetrični fluks sta bila prikazana grafično, njuna stopnja podobnosti pa je bila primerjana in statistično potrjena. Študija osvetljuje učinkovito recikliranje natrijevega lignosulfonata iz odpadne tekočine s pomočjo ultrafiltracije.



Except when otherwise noted, articles in this journal are published under the terms and conditions of the Creative Commons Attribution 4.0 International License